

Effects of Lipid Chain Length and Unsaturation on Bicelles Stability. A Phosphorus NMR Study

Mohamed N. Triba, Philippe F. Devaux, and Dror E. Warschawski

Unité Mixte de Recherche No. 7099, Centre National de la Recherche Scientifique, Institut de Biologie Physico-Chimique, Paris, France

ABSTRACT Most studies reported until now on the magnetically alignable system formed by the binary mixtures of long- and short-chain lipids were based on the mixture of 1,2-dimyristoyl-*sn*-glycero-3-phosphocholine (D14PC) and 1,2-dihexanoyl-*sn*-glycero-3-phosphocholine (D6PC) lipids. We have recently shown that a large part of the phase diagrams of this lipid mixture could be understood by taking into account the partial miscibility between the long-chain lipids and the short-chain lipids when the sample was heated above the melting transition temperature (T_m) of the long-chain lipids. In this work, we show by modifying the chain length of either one of the two lipids that it is possible to control their miscibility and thus the intervals of temperature and composition where spontaneous alignment is observed in a magnetic field. By using ^{31}P NMR, we demonstrate that the very special properties of such binary lipid mixtures are correlated with the propensity for short-chain lipids to diffuse into the bilayer regions. We also show that lipid mixtures with comparable properties can be formed with unsaturated lipids such as 1-palmitoyl-2-oleoyl-*sn*-glycero-3-phosphocholine (POPC).

INTRODUCTION

The aqueous suspension composed by the mixture of short-chain lipids and long-chain lipids was studied by Roberts et al., in the 1980s (1–7). They inferred the existence of disk-like micelles, usually named bicelles, which formed below the main transition temperature of the long-chain lipid T_m . Throughout this article, the word bicelle will refer to a disk-shaped aggregate. Above T_m , depending on temperature and composition, various lipidic structures are formed. As demonstrated by Sanders and Schwonek in the early 1990s (8), one of the most interesting properties of this binary mixture is its ability to spontaneously align in a magnetic field. However the topology of the lipid aggregates formed at the temperature and composition conditions where alignment is observed is still debated (9–19).

Although this lipidic system is mostly used to partially orient soluble proteins and measure residual dipolar couplings that provide structural constraints in liquid-state NMR (20–22), it was first considered a good membrane mimic for structural studies of membrane proteins (8). The approach was comparable to the study of membranes mechanically aligned on glass plates but with a much higher level of hydration allowing one to play with pH, ionic strength, and temperature (23,24). This idea was also appealing since native structure and activity of proteins seemed to be better preserved when incorporated in this membrane mimic (25,26) than in detergent micelles (27). This approach was successfully applied to small membrane proteins (25,28–34),

and we have recently demonstrated that it can also be used for larger membrane proteins (~ 20 kDa) (35).

Since the work of Sanders and co-workers, most reports on the binary mixture of a long- and a short-chain lipid have focused on systems composed of 1,2-dimyristoyl-*sn*-glycero-3-phosphocholine (D14PC) as long-chain lipids and 1,2-dihexanoyl-*sn*-glycero-3-phosphocholine (D6PC) as short-chain lipids. One can wonder whether this composition is optimal for the study of membrane or soluble proteins. Several empirical attempts have already been performed by other laboratories, and it was shown that lipids with various acyl chains, backbones, or headgroups could be used (36–40). In this work, we have determined how the variation of lipid chain length and the presence of unsaturated lipids could modify the properties of the lipid suspension. We have done so by varying both the temperature and the molar ratios q between long- and short-chain lipids. Special attention was given to the temperatures and q range where spontaneous lipid alignment was observed. In particular, we have studied the correlation between the alignment property and the propensity for short-chain lipids to diffuse into the domains containing a majority of long-chain lipids.

MATERIALS AND METHODS

Sample preparation and manipulation

1,2-dipentanoyl-*sn*-glycero-3-phosphocholine (D5PC), 1,2-dihexanoyl-*sn*-glycero-3-phosphocholine (DHPC or D6PC), 1,2-diheptanoyl-*sn*-glycero-3-phosphocholine (D7PC), 1,2-dilauryl-*sn*-glycero-3-phosphocholine (DLPC or D12PC), 1,2-dimyristoyl-*sn*-glycero-3-phosphocholine (DMPC or D14PC), 1,2-dipalmitoyl-*sn*-glycero-3-phosphocholine (DPPC or D16PC), and 1-palmitoyl-2-oleoyl-*sn*-glycero-3-phosphocholine (POPC) were purchased from Avanti Polar Lipids (Alabaster, AL). Samples were prepared as described previously (17). In this article, samples are prepared for a final lipid concentration in water c_1 of 25% (w/w).

Submitted March 15, 2006, and accepted for publication May 5, 2006.

Address reprint requests to Dror E. Warschawski, Institut de Biologie Physico-Chimique, 13 rue Pierre et Marie Curie, 75005 Paris, France. Tel.: 33-1-58-41-51-11; Fax: 33-1-58-41-50-24; E-mail: dror.warschawski@ibpc.fr. Mohamed N. Triba's present address is Oxford Biomembrane Structure Unit, Biochemistry Department, University of Oxford, South Parks Rd., Oxford, OX1 3QU, UK.

© 2006 by the Biophysical Society

0006-3495/06/08/1357/11 \$2.00

doi: 10.1529/biophysj.106.085118

NMR experiments

Experiments were carried out on a Bruker AVANCE DMX 400-WB spectrometer (Wissembourg, France) with a 9.7 tesla field. The corresponding frequency for ^{31}P nuclei is 162 MHz. The insert that contains the sample is inserted in a classical outer NMR tube with a diameter of 10 mm (New Era Enterprises, Vineland, NJ). The outer tube contained D_2O to allow us to lock the spectrometer field during acquisition. It also contained, in some instances, a phosphate solution the signal of which is used as a frequency reference that we have fixed at 2 ppm. The position of the narrow line associated to isotropically tumbling micelles is then -1 ppm. The variation with temperature of this reference was tested and was found very small. ^{31}P (90°) pulses were obtained in $26 \mu\text{s}$. To avoid heating the sample, we used a very low ^1H continuous decoupling power (6 kHz). Hahn echo pulses were used with a delay of $40 \mu\text{s}$. The delay between each cycle was 5 s. Spectra were recorded from low to high temperature. For each spectrum, 128 acquisitions were collected. The delay between acquisitions was 20 min.

RESULTS

Variation of the length of the short-chain lipids

^{31}P -NMR data were obtained with several binary lipid mixtures, which only differ by the chain length of the short lipids: D14PC/D5PC and D14PC/D7PC. For each mixture the molar ratio, q , between the long-chain lipids and the short-chain lipids was varied from $q = 3$ to $q = 12$. In Fig. 1, we compare the temperature variation of ^{31}P NMR spectra obtained at $q = 3$ and $q = 6$ for the two lipid mixtures.

Lipid molar ratio: $3 \leq q < 6$

As observed previously for the D14PC/D6PC mixture (17), three different temperature ranges can be defined for q values for which sample alignment is deduced ($2.5 < q < 6$). Under T_m , the main transition temperature of the long-chain lipid, the samples are fluid and transparent and only isotropic resonances are observed. Between T_m and a critical temperature named T_v , the samples are very viscous but still transparent: two, and only two, aligned signals are observed. Above T_v , the samples become milky but less viscous, and an isotropic signal coexist with resonances around -15 ppm. It is also observed at $q = 4$ and $q = 5$ for the two mixtures (D14PC/D5PC and D14PC/D7PC) studied here (data not shown).

At temperatures below T_m , two resonances coexist around -1 ppm. As previously shown for the D14PC/D6PC mixture, the signal at high field can be assigned to the long-chain lipids, whereas the signal at low field can be assigned to the short-chain lipids. In the inset above Fig. 1 *a*, we observe that the D5PC signal is sharper than the D14PC signal, indicating a faster molecular reorientation for the short-chain lipids. It is more difficult to discriminate both signals for the D14PC/D7PC mixture (see the asymmetry in the inset above Fig. 1 *c*). This is probably a consequence of a slower reorientation of D7PC compared to D6PC or D5PC.

In the intermediate temperature domain, we note a few differences between the two mixtures in this range of q values. i), The onset of the alignment can be observed at a much lower temperature for the D14PC/D7PC than for

the D14PC/D5PC mixture. For $q = 3$, we measured a 20° mosaicity at 28°C for the D14PC/D7PC mixture, whereas for the D14PC/D5PC mixture the sample was heated until 38°C to reach the same level of alignment. As previously observed (17), the temperature at which the onset of alignment is observed also decreases with q . ii), At the same temperature, the frequency of the signal assigned to the long-chain lipid is at a higher field for the D14PC/D7PC than for the D14PC/D5PC mixture. This indicates a better alignment of the mixture containing D7PC. If we consider that the bilayer normal oscillates rapidly in a cone, we can calculate the aperture of this cone by using a Gaussian distribution of the different orientations. For the D14PC/D7PC and the D14PC/D5PC mixtures, we find an aperture of 17° and 21° , respectively, at 42°C . iii), For this intermediate domain, relatively to the frequency of the long-chain lipid, the frequency of the short-chain lipid stays much closer to the isotropic frequency (-1 ppm) for the D14PC/D5PC than for the D14PC/D7PC mixture.

For higher temperatures ($T > T_v$), the signals around -15 ppm are much more important for the D14PC/D7PC than for the D14PC/D5PC mixture. As expected, the spectral properties that were previously observed for the D14PC/D6PC mixture are intermediate compared to those observed for the two mixtures studied here.

Lipid molar ratio: $q \geq 6$

Below T_m , ^{31}P NMR spectra are composed of isotropic lines corresponding to the short-chain and long-chain lipids. Since the line widths of these resonances increase with q , they can hardly be discriminated for $q \geq 6$ (see the asymmetry in the insets above Fig. 1, *b* and *d*). For $q > 6$, in addition to these isotropic components, a broad signal characteristic of long-chain lipid bilayers in gel phase appears in this temperature domain (data not shown). Above T_m and for high q values, the signal observed for D14PC/D7PC differs considerably from that of D14PC/D5PC. For example, in this temperature range, no isotropic peak is present at -1 ppm for the D14PC/D7PC mixtures, whereas a small isotropic peak is observed at all temperatures for the D14PC/D5PC mixtures. For both mixtures, two asymmetric signals appear just above T_m . Signal integration indicates that the high and low field resonances can be assigned, respectively, to the long- and short-chain lipids. These two signals tend to get closer when the temperature is increased. For the D14PC/D7PC mixture, both lines overlap and, at high temperature, only one line remains around -15 ppm, suggesting a total miscibility of the two lipids. For the D14PC/D5PC mixture, these two aligned signals stay apart for $q \leq 10$ even when the sample is heated over 60°C .

Variation of the long-chain lipids

We consider now the results obtained with two mixtures that only differ by the chain length of the long lipids: D12PC/D6PC and D16PC/D6PC. Here again, the molar ratio q was varied from $q = 3$ to $q = 12$. In Fig. 2, we compare results

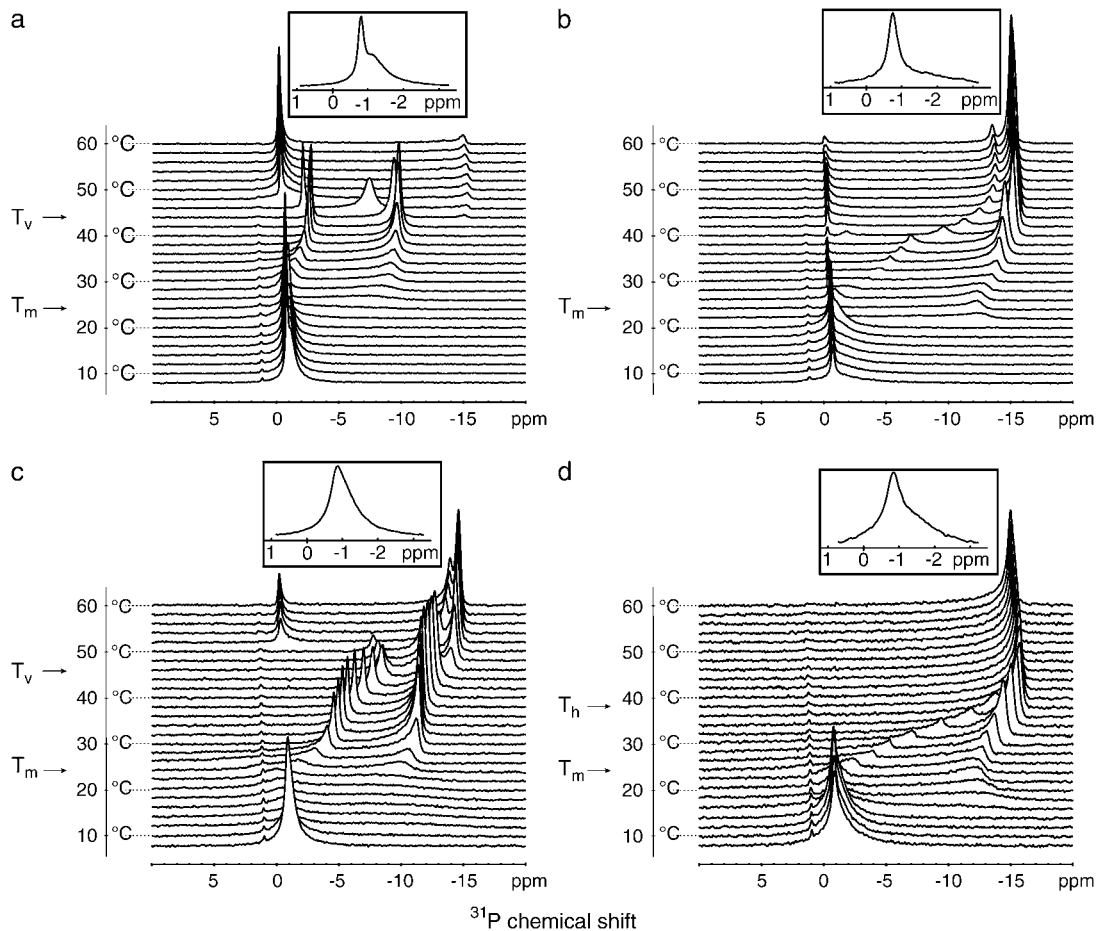


FIGURE 1 ^{31}P -NMR spectra at 162 MHz of mixtures D14PC/D5PC (*a* and *b*) and D14PC/D7PC (*c* and *d*) at temperatures between 8°C and 60°C. q values were, respectively, 3 (*a* and *c*) and 6 (*b* and *d*). A line broadening of 10 Hz was applied before Fourier transformation. Insets above the figures correspond to the isotropic region of spectra obtained at 8°C.

obtained at $q = 3$ and $q = 6$ for the two lipid mixtures at different temperatures.

Lipid molar ratio: $3 \leq q < 6$

As observed for other mixtures in this range of molar ratio, q , three temperature domains are observed for the D16PC/D6PC mixtures. Because the main transition T_m of D12PC is at low temperature (-1°C), no spectra can be recorded below T_m for this sample. However, above T_m the behavior of this mixture is qualitatively similar to that of other mixtures.

The most important difference between the signals recorded for the D16PC/D6PC and the D12PC/D6PC mixtures is the size of the temperature domain where alignment is observed. As observed for other mixtures, the onset of the alignment is located slightly above the main transition temperature, T_m , of the long-chain lipid. Consequently, the onset of alignment can be observed at a much lower temperature for the mixture that contains D12PC ($T_m = -1^\circ\text{C}$) than for the mixture that contains D16PC ($T_m = 41^\circ\text{C}$). For $q = 3$, we measured a 20° mosaicity at 22°C for D12PC/D6PC, whereas for the

D16PC/D6PC mixture, the samples were heated up to 44°C to reach the same level of alignment. The critical temperature, T_v , above which a signal appears around -15 ppm, is higher for the D12PC/D6PC mixture than for the D16PC/D6PC mixture. We found that for $q = 3$, $T_v = 52^\circ\text{C}$ for the former mixture and $T_v = 46^\circ\text{C}$ for the latter.

Lipid molar ratio: $q \geq 6$

For each mixture the different signals tend to overlap around -15 ppm when the sample is heated above T_m . However, the complete overlapping takes place much more rapidly for the D16PC/D6PC mixture than for the D12PC/D6PC mixture. This indicates that, relative to T_m , the short-chain lipids and the long-chain lipids mix totally at a lower temperature for the D16PC/D6PC mixture than for the D12PC/D6PC mixture.

Long-chain/short-chain lipid mixtures containing unsaturated long-chain lipids

We have prepared mixtures of short-chain and long-chain lipids with different proportions of POPC, a long-chain lipid

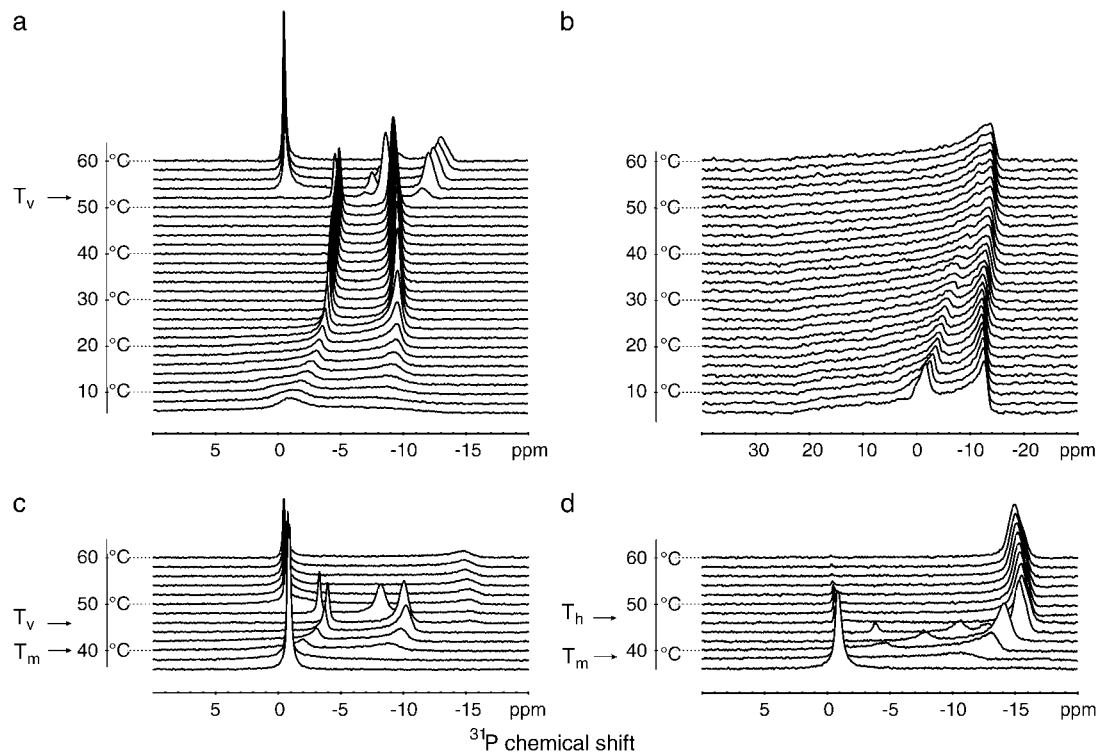


FIGURE 2 ^{31}P -NMR spectra at 162 MHz of D12PC/D6PC (*a* and *b*) D16PC/D6PC (*c* and *d*) mixtures at temperatures between 8°C and 60°C. q values were, respectively, 3 (*a* and *c*) and 6 (*b* and *d*). A line broadening of 10 Hz (50 Hz for (*b*) spectra) was applied before Fourier transformation.

with one unsaturation on the *sn2* chain. In Fig. 3, *a* and *b*, we show ^{31}P NMR spectra obtained with D14PC/POPC/D6PC mixtures with a composition of 2.6/0.4/1 and 1.5/1.5/1, respectively. No alignment is observed when the proportion of POPC is larger than the proportion of D14PC. Integration of the two NMR signals observed when the samples are aligned indicates that POPC and D14PC signals resonate at the same frequency (the high field signal), whereas the low field signal can be assigned to D6PC. Since these two long-chain lipids have the same headgroup, this shows that the level of alignment is the same for POPC and D14PC. We also observe that, in the presence of POPC, the temperature range where alignment takes place is shifted toward low temperatures. This shift increases with the POPC/D14PC molar ratio. For the 2.6/0.4/1 and 1.5/1.5/1 samples, the alignment onset is observed at, respectively, 21°C and 15°C, whereas the critical temperatures, T_v , are situated at, respectively, 35°C and 23°C.

DISCUSSION

In the first part of this section, we discuss the temperature variation of the miscibility between long- and short-chain lipids for the different mixtures and we examine the structural consequences. Then, we discuss the influence of a chemical modification of the lipids. Finally, we analyze the different structural models proposed for the temperature range where sample alignment is detected. In particular, we

discuss the specific consequences of the miscibility variation for the perforated lamellae model.

Structural consequences of the variation of lipid miscibility with temperature

Concentrated samples ($c_1 > 5\%$ (w/w)) with q ranging between 2.5 and 6 were particularly studied because they have the unique property of aligning spontaneously in the magnetic field above T_m . For these concentrations and q range, it is now largely admitted that discoidal structures are formed below T_m . At these temperatures the disk bilayer is in gel state and contains only a negligible fraction of short-chain lipids (6,7,11–14,16,18,19). This segregation at low temperature is also in agreement with observations made for other binary lipid mixtures (41–43).

Above the main transition temperature, T_m , of the long-chain lipid, the physical properties of the bicellar suspension change dramatically. In particular, the sample apparent viscosity rapidly increases and, for $2.5 \leq q \leq 6$, spontaneous alignment is observed in a magnetic field. Different structures are proposed in this q and temperature range: disks, perforated lamellae, or ribbons. Whatever the topology of these alignable objects, we have shown that the increase in lipid miscibility is the driving force for structural changes observed when the temperature is increased above T_m . The ideal bicelle proposed by Vold and Prosser (9) for these

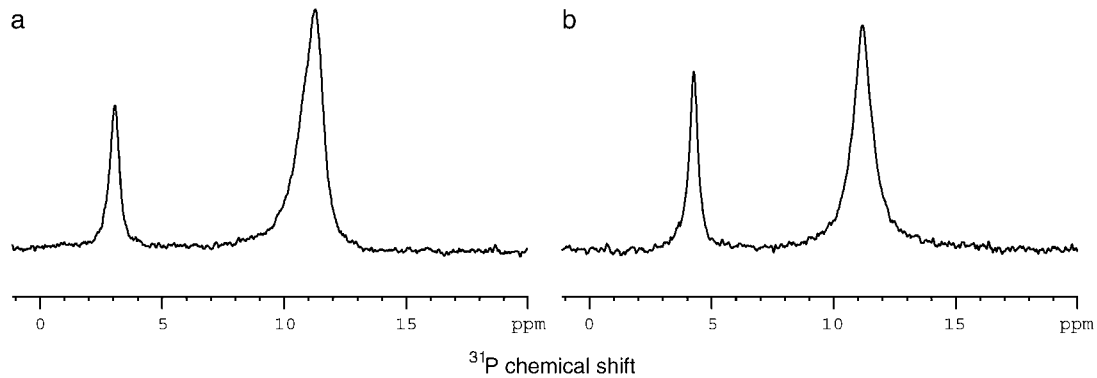


FIGURE 3 ^{31}P -NMR spectra at 162 MHz of D14PC/POPC/D6PC mixtures with molar compositions of 2.6/0.4/1 (a) and 1.5/1.5/1 (b). The spectra were recorded at 23°C (a) and 22°C (b), respectively. A line broadening of 10 Hz was applied before Fourier transformation.

temperatures, where short-chain and long-chain lipids would be totally segregated, is incompatible with most phase diagrams of lipid/lipid mixtures (42,44,45) and with entropic considerations (46). The miscibility variation that we have measured previously for the D14PC/D6PC mixture (17) induces an important edge shrinkage and an important bilayer increase. This bilayer increase can explain the orientability of the structures formed above T_m . The rapid edge decrease relative to the bilayer domains also explains the formation of vesicles at very high temperatures.

Using Sanders's approach (8), which assumes a fast exchange between the short-chain lipids located, respectively, in the long-chain-rich section and in the short-chains-rich section, we have shown that the temperature variation of ε (i.e., fraction of short-chain lipids inside the long-chains-rich section) can be deduced using ^{31}P NMR frequencies of the two different lipids (17). In our previous work, we have shown for D14PC/D6PC that, for a given temperature, the ratio between the short- and the long-chain lipid resonance frequencies varies linearly with the molar ratio q and that ε can be deduced from the linear fit. This linear variation is also

observed for the mixtures studied here (data not shown). In Fig. 4, we show the deduced ε values. For comparison, results obtained with the D14PC/D6PC mixtures are also plotted.

As observed previously, the miscibility of the short-chain lipids in the bilayer rapidly increases above the main transition temperature of the long-chain component. Because of the important mismatch between the long and the short chains, this miscibility remains relatively small, as suggested by the absence of crosspeaks between D6PC and D14PC in a nuclear Overhauser effect spectrum (47). This phenomenon has very important structural consequences. The proportion of bilayers relative to the proportion of edges can be represented by the volume ratio, q_v , between these two domains, and q_v can be estimated using the following expression (17):

$$q_v \approx \frac{q}{\lambda} \left[\frac{1 + \varepsilon(\lambda - 1)}{1 - \varepsilon(q + 1)} \right], \quad (1)$$

where λ is the ratio between the volume of a short-chain lipid and the volume of a long-chain lipid.

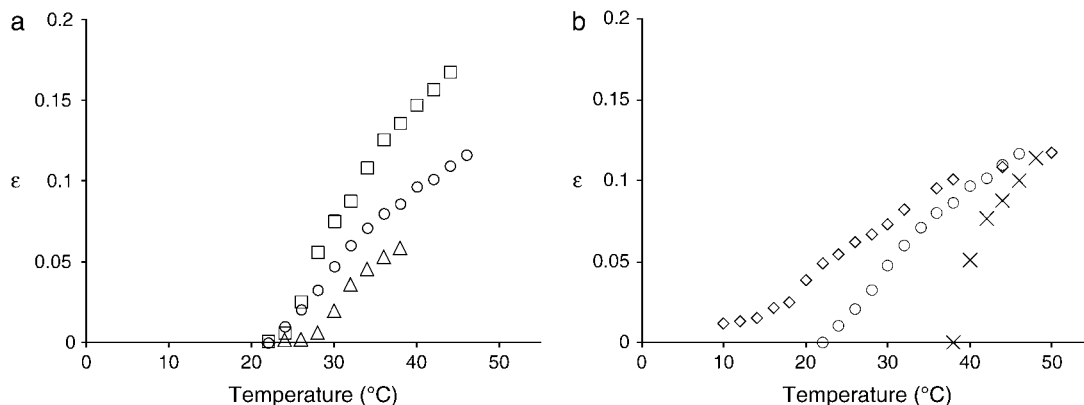


FIGURE 4 Molar fraction ε of short-chain lipids in the bilayer section as a function of temperature. These values are deduced from the ^{31}P NMR spectra as explained in (17): (a) D14PC/D7PC (squares) and D14PC/D5PC (triangles) mixtures. (b) D12PC/D6PC (diamonds) and D16PC/D6PC (crosses) mixtures. For the sake of comparison, results obtained with the D14PC/D6PC mixture are also presented (circles).

Fig. 5 presents the temperature variation of q_v for $q = 2$ and $q = 4$ in the case of the D14PC/D7PC mixture. Fig. 5 shows that the proportion of bilayer increases rapidly with temperature for q values for which spontaneous alignment is observed. For $q = 4$, the volume ratio between bilayers and edges is multiplied by 7 between 23°C and 45°C. In agreement with Eq. 1, the larger q is, the steeper the increase is. Since the ability for a lipidic aggregate to align in the magnetic field increases with the proportion of bilayer (48), the temperature at which the onset of spontaneous alignment takes place should decrease when q increases. This is what we observe experimentally. At very high temperatures, alignable structures are no longer stable and they are replaced by perforated vesicles (17). The edge domain shrinking, due to short-chain lipids relocating in the bilayer section when the sample is heated, explains the structural transition. q_v expression (Eq. 1) also indicates that the larger q , the faster the edge shrinkage when ε increases. Therefore, the alignment loss and the formation of a milky phase, characteristic of lipidic vesicles, are observed at lower temperatures when the proportion of long-chain lipids in the sample is increased.

For small q values ($q < 2.5$), the proportion of bilayer remains small at all temperatures studied. Consequently, for such samples, no alignment is observed and vesicles are formed only at very high temperatures ($>50^\circ\text{C}$), as noted previously by Nieh et al. (15). Here again the partial miscibility between the two lipids provides a simple explanation for the strong q dependence of T_v (17).

Influence of the length of the short-chain lipids

Fig. 4 *a* presents the variation of ε with temperature when the short-chain lipid length is varied. The length of the short chains strongly influences the demixion of the two lipids. For a given temperature above T_m , D5PC is much less mis-

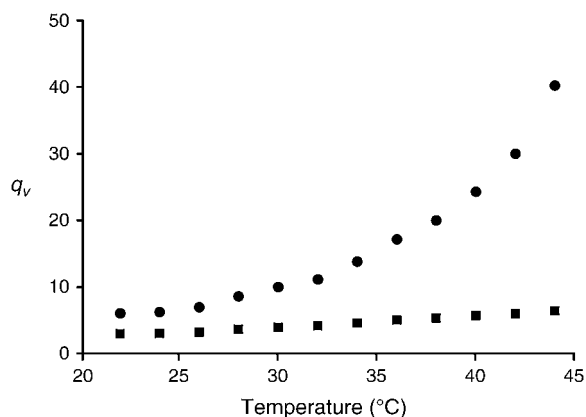


FIGURE 5 Volume ratio between the bilayer section and the edge section as a function of temperature for the D14PC/D7PC sample. The values are obtained for $q = 2$ (squares) and $q = 4$ (circles) using Eq. 1 and experimental values of ε (see Fig. 4). The volumes of D7PC and D14PC molecules are, respectively, 714 \AA^3 and 1090 \AA^3 (65), so that $\lambda = 0.66$.

cible in the D14PC-rich domain than D7PC. D6PC exhibits an intermediary behavior. This is in agreement with previous results obtained with other lipids mixtures where it was shown that the miscibility increases when the mismatch between lipid chain lengths decreases (41–43).

Since the samples studied here are very concentrated ($c_1 = 25\%$ (w/w)), we have neglected the amount of D7PC- or D6PC-free monomers. However, because of the large value of D5PC critical micellar concentration, we cannot exclude that a nonnegligible fraction of D5PC is present as monomers in the D14PC/D5PC samples that we have studied. In this case the sample is composed of three chemical elements and separated into three domains: a D14PC-rich domain (the bilayers), a D5PC-rich domain (the edges), and the water-rich domain (the bulk water). The D5PC ^{31}P NMR signal is then an average of the “instantaneous” signals of this molecule respectively in the bilayer, the edge, or the bulk water. The method used to determine ε was first applied to a system where the short-chain lipids exchanged between two domains (bilayers and edges). However, this method is still valid for the D14PC/D5PC mixture since Gibbs laws impose that, as long as these three domains coexist, the composition of each domain depends on the temperature but not on the molar ratio, q . Since lipids in edges or in bulk water are less ordered than those in bilayer regions, the small proportion of D5PC determined in the bilayer (Fig. 4 *a*) is in agreement with the NMR signal of this lipid, remaining very close to the isotropic frequency (-1 ppm). In Fig. 1 *b*, an isotropic signal is present at all temperatures studied for the D14PC/D5PC mixture. The nonnegligible proportion of free D5PC in water can explain this observation. The steeper ε increase for D14PC/D7PC compared to D14PC/D5PC implies that the proportion of lipids that form bilayers becomes rapidly more important for the first mixture. This result confirms that spontaneous alignment is better and takes place more rapidly for D14PC/D7PC than for the D14PC/D5PC mixture when the temperature is increased above T_m (Fig. 1, *a* and *c*).

In Fig. 1 *d* we clearly see that the long-chain and the short-chain signals tend to get closer when the D14PC/D7PC sample is heated and overlap at 38°C . This indicates that the fraction of short-chain lipids available for edge regions is progressively reduced until only bilayer regions remain. This phenomenon is much less pronounced for D14PC/D5PC, even for samples with larger q values or temperatures. This difference between the two samples is also a consequence of the different miscibility of D5PC and D7PC in the bilayer.

Influence of the length of the long-chain lipids

Fig. 4 *b* presents ε as a function of temperature when the long-chains lipid length is varied. For mixtures that contain D14PC or D16PC, the temperatures at which the onset of miscibility is observed correspond to the main transition temperatures of the long-chain lipids (respectively, 22°C and 41°C). For mixtures that contain D12PC, no measurements

were made at T_m because it is below the ice-water transition temperature. However, our results indicate that the hydrophobic chain disorder of the long-chain lipids is a requirement for miscibility as well as for alignment. The increase of miscibility with temperature is faster when the long-chain lipid is longer. To compare bilayers composed of lipids that have different main transition temperatures, Seelig and Browning have proposed using a reduced temperature $T_r = (T - T_m)/T_m$ (49). They showed that this reduced temperature is characteristic of the hydrophobic chain disorder. If we use this temperature scaling, for a given value of the reduced temperature the miscibility of the short-chain lipid in the bilayer increases with the length of the long-chain lipid (not shown).

ε is determined by the relative affinity of the short-chain lipid for the edges and for the bilayer domains. Whereas the affinity for the bilayer domain is increased when the mismatch between the two lipids is reduced, the affinity for the edge is determined by the compatibility between the geometry of the short-chain lipid and the geometry of this domain. There is a strong link between the lipid shape and the more favorable shape of the aggregate formed by this lipid (50). The curvature at the hydrophilic/hydrophobic interface of the edge is constrained by the necessity for the short-chain lipids to totally cover the hydrophobic domain of the bilayer. However, in the more favorable case, this curvature should be close to the average curvature at the hydrophilic/hydrophobic interface of D6PC micelles ($92 \times 10^{-3} \text{ \AA}^{-1}$; (51)). Thus, the affinity of the short-chain lipids for this domain should be dependent on the bending energy involved in forming one edge (see supplementary material). Even though ε is largely affected by the value of T_m , the steeper miscibility increase with temperature when the long-chain lipid is longer is probably a consequence of the variation of D6PC affinity for edges.

In Fig. 2, *a* and *c*, the temperature range for which alignment is observed is much larger for D12PC/D6PC than for D16PC/D6PC. This difference is a direct consequence of the variation of miscibility with temperature. The increase of ε with temperature induces a shrinking of the edge and a transition from aligned structures to perforated vesicles. If ε increase is slow with temperature, this shrinking of edges is slow and the temperature range for which alignment is observed is large. On the contrary, if ε variation is fast, the temperature range for which alignment is observed is small. This result demonstrates that the ability of the lipidic mixture to form alignable structures is directly related to the propensity of short-chain lipids to diffuse into the bilayer region. Thus, alignable structures can exist only when the miscibility is comprised between zero and a critical value that corresponds to the transition to perforated vesicles.

Influence of the unsaturated lipids

In agreement with a recent report by the Lorigan group (52), we have shown here that alignment in the magnetic field can

also take place when long-chain unsaturated lipids are present in the lipidic mixture. An interesting effect of unsaturated lipids is that the temperature range where alignment is observed is shifted toward low temperatures. As mentioned previously, alignment is observed only when the lipid bilayer is in the fluid phase. When only one class of long-chain lipids is mixed with short-chain lipids, alignment is always observed above the main transition temperature of this long-chain lipid (Figs. 1, *a* and *c*, and 2, *a* and *c*; (17)). The long-chain lipid fluidity is also required for the lateral diffusion of the short-chain lipids inside the bilayer domain. Thus, the shift of temperature range where alignment is observed indicates that the addition of unsaturated lipids decreases the lowest temperature for which the bilayer is in fluid phase. The variation of this temperature shift with the POPC/D14PC molar ratio is in agreement with the POPC/D14PC phase diagram (53).

Structural and geometrical considerations

To increase the efficiency of membrane protein studies with this membrane mimic, we believe that we also need a better geometrical description of the lipidic structure formed in temperature and composition ranges where alignment is observed. Three types of lipidic structures are proposed for this phase diagram domain. The first structure suggested was bicelles (8). A few years later, different groups suggested that the alignable structure was composed of stacked perforated bilayers (10,13,14) or ribbons, also called wormlike or flattened cylindrical micelles (15,18,19). The three structures contain long-chain-lipid-rich domains (bilayers) and short-chain-lipid-rich domains (edges) and can explain at first approximation the ^{31}P NMR spectra obtained when the lipidic structure is aligned.

Geometrical considerations of the perforated lamellae model

In a monodisperse solution, the bicelle radius or the ribbon width are roughly given by $r_{\perp} q_v$, where r_{\perp} is the edge thickness (see Supplementary Material). However, in the perforated lamellae model, even if q_v is known, the assumption of monodispersity of the pore size is not sufficient to estimate the pore radius or the average distance between pores. Based on a similar geometrical approach than the one used by Holmes and co-workers in their studies of mesh phases (54), we propose a formula to estimate the radius of pores, R_p , in the perforated lamellae model (see Fig. 6 and Supplementary Material). With this model, we find a pore radius, R_p , of 416 Å. Knowing the pore radius, we estimate the distance, d_p , between the edges of two adjacent pores by considering a homogeneous distribution of pores at the perforated lamellae surface (see Supplementary Material). We find a distance, d_p , between pores of 170 Å. Thus, in the perforated model, the distance between pores should be, on average, five times smaller than the pore diameter. This

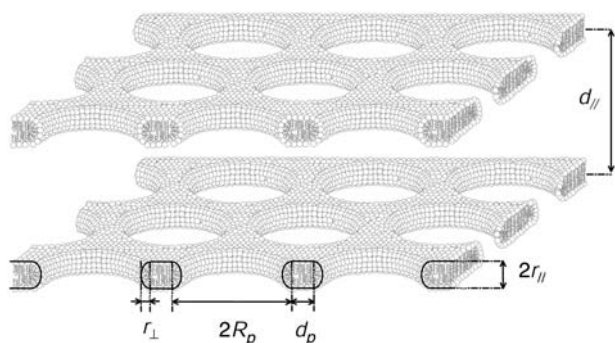


FIGURE 6 Schematic representation of stacked perforated bilayers. In the simplified model presented here, the bilayers are uniformly perforated; all the pores are circular and have the same size. Distances indicated in this figure are explained in the text and in the supplementary material.

perforated structure could be seen as small lipidic domains connected by thin lipidic ribbons or wormlike micelles. Because of the very small value of the ratio d_p/R_p , one pore cannot diffuse between two other pores without interacting with them. As a consequence of their very high surface density, diffusion of pores in the lamellae should lead to frequent and transient fusions and breakdowns of the thin lipidic ribbons that connect bilayer sections. In that case, it becomes merely a semantic issue to call these objects perforated lamellae rather than disks or ribbons arranged onto planes and transiently interconnected.

Recently, van Dam et al. (19) have published a work confirming the increasing lipid miscibility with temperature (17,55). Cryo-electron microscopy shows some structures obtained in the region where bicellar mixtures align in a magnetic field. Although other micrographs show evidences of disks (56), these micrographs support our hypothesis here that perforated lamellae are so highly perforated that they can hardly be called lamellae, let alone Swiss cheese. Cylindrical micelles just above T_m , as suggested by van Dam et al. (16,19), would require a sudden increase in lipid miscibility, followed by a decrease in lipid miscibility with temperature. This would contradict all physicochemical data on lipid mixtures. On the other hand, disks interacting on an edge-on manner can, to some extent, be called ribbons (15).

Comparison between perforated lamellae and disks arranged onto planes

Different experiments were performed to support the perforated lamellae model. It was suggested that the perforated lamellae model could explain the results obtained by small angle neutrons scattering (13,14,18). However, scattering studies alone are not always sufficient to discriminate between different structures formed by aggregated lipids (57). Furthermore, if we consider the Babinet principle, results obtained by Katsaras and co-workers can also be interpreted as disks arranged onto planes (58).

The perforated lamellae model was also supported by NMR diffusion studies. It has been shown, for example, that the lateral diffusion of lipophile molecules measured by NMR is more important above than below T_m (10,59,60). However, lateral diffusion in a lipid bilayer is always more important when this bilayer is in the fluid phase than in the gel phase. Whatever the structural model proposed, this can also explain why the lateral diffusion of lipophile molecules is limited below T_m in the bicellar systems. Furthermore, as suggested by Gaemers and Bax (10), these experiments can also be explained by disks making transient contacts in an edge-on manner. If we replace perforated lamellae by disks arranged onto planes, we can calculate the average distance between the edges of two neighboring disks by using the same approach as the one used to estimate the pore radius and the distance between pores (see supplementary material). We find a disk radius, R_d , of 260 Å and an average distance, d_d , of 256 Å between edges of two neighboring disks. If one approximates the lateral diffusion of these bicelles by the lateral diffusion of a sphere of 260 Å radius, we can calculate that it takes $<40 \mu\text{s}$ for a bicelle to diffuse until it collides with the closest neighbor (see supplementary material). This result suggests that lateral diffusion of lipophilic molecules between disks interacting in an edge-on manner cannot be excluded since diffusion measured by NMR takes place during diffusion times on the order of several hundreds of milliseconds, a very long time compared to the time needed for a disk to diffuse until it makes contact with the closest neighbor.

Finally, to explain the fact that the ^{31}P NMR frequency of the bilayer signal is not ~ -15 ppm, as expected for a perfectly oriented membrane, one has to assume that the perforated lamellae surface undulates rapidly on the ^{31}P NMR timescale ($\tau_c \approx 10^{-6}$ s). These undulations must be much faster than the undulations observed at the surface of classical lipidic membranes, whose characteristic time is on the order of the millisecond (61). Fast reorientation of the bilayer domains can easily be explained by considering small disks oscillating around their average orientation.

Although they appeal to physicists, structural models such as perfect perforated lamellae, perfect disks arranged onto planes, or perfect ribbons fail to give an explanation for all the experimental observations without considering local transient interactions between bilayer sections. If we consider, for example, the very high density of pores that should exist in perfect perforated lamellae or the very short time needed for a perfect disk to interact with its neighbors, we can deduce that the real structure is an intermediate structure between perfect geometrical models proposed until now. Locally, rapid fusion and breakdown of bicelles can lead to formation of transient pores as well as intermediary structures such as noncircular disks or pores. These noncircular disks or pores are favored when the lipidic domains are fluids ($T > T_m$) because the line tension at their interface is smaller than when the bilayer domain is in the gel phase ($T < T_m$). Hare

and co-workers have shown that more than 10^7 lipids have to interact to reach alignment (48), which is much larger than the few thousand lipids that form a disk. Since interconnection between disks would increase the number of lipids interacting cooperatively with the magnetic field, it would explain the alignment as well as the viscosity increase when alignment is observed. Finally, transient interactions between small bilayer domains would allow their fast oscillations observed around their average orientation ($\tau_c \ll 10^{-6}$ s), compared to the slow undulation expected for a perfect bilayer ($\tau_c \approx 10^{-3}$ s).

From unstable perforated lamellae to stable perforated vesicles

We have shown that perfect perforated lamellae were unlikely to be stable in the temperature domain where alignment takes place in the magnetic field. On the other hand, the formation of perforated vesicles can account for the different experimental results obtained at higher temperatures, where the alignable structures collapse (15–19,62). To explain the formation of these stable perforated structures, we can use the formulae obtained for perfect perforated lamellae and study their variation when the temperature or the miscibility between the two lipids increases (Fig. 7). Since d_p strongly increases when the short-chain lipids diffuse into the bilayers, increasing the temperature should increase the stability of perforated structures. In other words, when the temperature increases, the short-chain lipids diffuse into the long-chain lipid-rich domains, the bilayer size rapidly increases relatively to the proportion of edges, and perforated structures become globally less perforated and thereby more stable. Our formulae cannot be used as such when aligned structures have collapsed. Above the transition temperature, T_v , a phase separation occurs between perforated vesicles and small

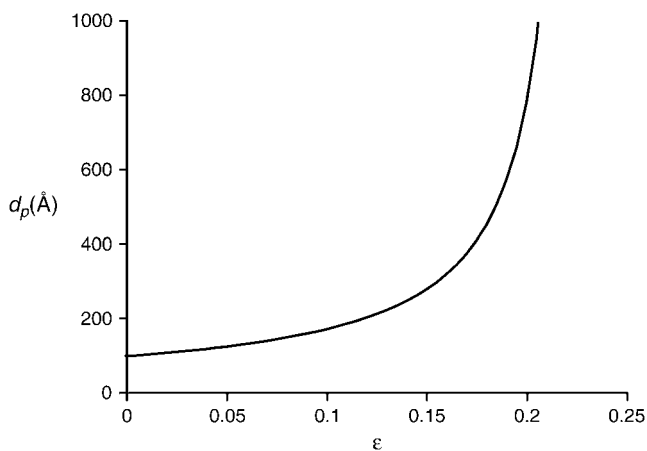


FIGURE 7 Theoretical variation of the distance, d_p , between the edges of two adjacent pores as a function of the mol fraction ε of D6PC in the bilayer section. This simulation is obtained for $q = 3.4$ by using Eq. S11 and the parameters explained in the Supplementary Material.

bicelles or micelles (17). The repeating distance between stacked bilayers in perforated vesicles is different from the repeating distance measured in the aligned structures (63). Thus, above T_v , the sample is not homogeneous anymore and the local values of ϕ_1 , d_p , and q_v in the perforated vesicles are different from the values used in the homogeneous aligned phase. Consequently, our formulae cannot be used to calculate structural dimensions in perforated vesicles above T_v . However, taken together, our results support the formation of stable perforated vesicles at high temperatures, when aligned structures have collapsed.

In summary, we can reconcile our results with those of van Dam et al. (19) by considering that disks formed below T_m start to interact in an edge-on manner above T_m , increase the viscosity, and align in a magnetic field. Then, progressively, as the size of the disk bilayer regions increase, collisions become more frequent and lead to two-dimensional networks of ribbons (or highly perforated lamellae) that align better and better. This evolution is gradual as neither ^{31}P NMR, diffusion studies, neutrons scattering, nor electron microscopy can detect a sharp transition. Finally, when the flat bilayer regions become too large at T_v , they bend and form (often perforated) vesicles (17,64).

CONCLUSION

In this report, we demonstrate that most of the remarkable properties of the bicellar mixture are preserved when the lipid chain lengths of both the long- and the short-chain lipids are modified by one or two carbons. We also demonstrate that these properties are maintained in the presence of a large fraction of unsaturated lipids such as POPC. However, our results show that the temperature domain where spontaneous alignment in a magnetic field is observed highly depends on the lipids used. In agreement with the mixed bicelle model (17), we show that the variation of this temperature domain can be controlled, as it is simply a consequence of the variation of miscibility between lipids. For a given temperature, this miscibility depends on the mismatch between chain lengths of the lipids, on the value of the main transition temperature of the long-chain lipid, and on the affinity of short-chain lipids for the edge sections. Furthermore, understanding the underlying forces that are responsible for the formation of alignable lipidic structures, we are able to predict which lipid mixtures would align and to design mixtures that would align in a desired specific temperature range. This is of particular interest for biological applications such as soluble protein partial orientation, membrane protein incorporation, or drug encapsulation (see supplementary material).

Considering the different structural models proposed for the temperature range where alignment is observed, we have also discussed the viability of the perforated lamellae model by proposing an analytical expression of the pore radius. Our results indicate that if perfect perforated lamellae were formed at temperatures where alignment is observed, they should be

highly perforated and probably very unstable. Without considering local but transient interactions between bilayer sections, no structural model proposed until now for the alignable structure can account for all the experimental observations. However, the analytical expression of a pore radius proposed in this report can explain the formation of stable perforated structures at high temperatures. Here again, this result demonstrates that the driving force of the structural changes observed when the sample is heated is the variation of the miscibility between the two lipids.

SUPPLEMENTARY MATERIAL

An online supplement to this article can be found by visiting BJ Online at <http://www.biophysj.org>.

The authors are very grateful to Jean-Pierre Duneau and Erwan Gueguen for initiating this project. The authors thank Thomas Zemb for helpful discussions.

This work was supported by the Centre National de la Recherche Scientifique and the Université Paris 7—Denis Diderot (UMR 7099).

REFERENCES

- Gabriel, N. E., and M. F. Roberts. 1984. Spontaneous formation of stable unilamellar vesicles. *Biochemistry*. 23:4011–4015.
- Gabriel, N. E., and M. F. Roberts. 1986. Interaction of short-chain lecithin with long-chain phospholipids: characterization of vesicles that form spontaneously. *Biochemistry*. 25:2812–2821.
- Gabriel, N. E., and M. F. Roberts. 1987. Short-chain lecithin/long-chain phospholipid unilamellar vesicles: asymmetry, dynamics, and enzymatic hydrolysis of the short-chain component. *Biochemistry*. 26:2432–2440.
- Gabriel, N. E., N. V. Agman, and M. F. Roberts. 1987. Enzymatic hydrolysis of short-chain lecithin/long-chain phospholipid unilamellar vesicles: sensitivity of phospholipases to matrix phase state. *Biochemistry*. 26:7409–7418.
- Eum, K. M., G. Riedy, K. H. Langley, and M. F. Roberts. 1989. Temperature-induced fusion of small unilamellar vesicles formed from saturated long-chain lecithins and diheptanoylphosphatidylcholine. *Biochemistry*. 28:8206–8213.
- Bian, J. R., and M. F. Roberts. 1990. Phase separation in short-chain lecithin/gel-state long-chain lecithin aggregates. *Biochemistry*. 29:7928–7935.
- Lin, T.-L., C.-C. Liu, M. F. Roberts, and S.-H. Chen. 1991. Structure of mixed short-chain lecithin/long-chain lecithin aggregates studied by small-angle neutron scattering. *J. Phys. Chem.* 95:6020–6027.
- Sanders 2nd, C. R., and J. P. Schwonek. 1992. Characterization of magnetically orientable bilayers in mixtures of dihexanoylphosphatidylcholine and dimyristoylphosphatidylcholine by solid-state NMR. *Biochemistry*. 31:8898–8905.
- Vold, R. R., and R. S. Prosser. 1996. Magnetically oriented phospholipid bilayered micelles for structural studies of polypeptides. Does the ideal bicelle exist? *J. Magn. Reson. B*. 113:267–271.
- Gaemers, S., and A. Bax. 2001. Morphology of three lyotropic liquid crystalline biological NMR media studied by translational diffusion anisotropy. *J. Am. Chem. Soc.* 123:12343–12352.
- Glover, K. J., J. A. Whiles, G. Wu, N. Yu, R. Deems, J. O. Struppe, R. E. Stark, E. A. Komives, and R. R. Vold. 2001. Structural evaluation of phospholipid bicelles for solution-state studies of membrane-associated biomolecules. *Biophys. J.* 81:2163–2171.
- Luchette, P. A., T. N. Vetman, R. S. Prosser, R. E. Hancock, M. P. Nieh, C. J. Glinka, S. Krueger, and J. Katsaras. 2001. Morphology of fast-tumbling bicelles: a small angle neutron scattering and NMR study. *Biochim. Biophys. Acta.* 1513:83–94.
- Nieh, M. P., C. J. Glinka, S. Krueger, R. S. Prosser, and J. Katsaras. 2001. SANS study on the structural phases of magnetically alignable lanthanide-doped phospholipid mixtures. *Langmuir*. 17:2629–2638.
- Nieh, M. P., C. J. Glinka, S. Krueger, R. S. Prosser, and J. Katsaras. 2002. SANS study on the effect of lanthanide ions and charged lipids on the morphology of phospholipid mixtures. *Biophys. J.* 82:2487–2498.
- Nieh, M. P., V. A. Raghunathan, C. J. Glinka, T. A. Harroun, G. Pabst, and J. Katsaras. 2004. Magnetically alignable phase of phospholipid “bicelle” mixtures is a chiral nematic made up of wormlike micelles. *Langmuir*. 20:7893–7897.
- Van Dam, L., G. Karlsson, and K. Edwards. 2004. Direct observation and characterization of DMPC/DHPC aggregates under conditions relevant for biological solution NMR. *Biochim. Biophys. Acta.* 1664:241–256.
- Triba, M. N., D. E. Warschawski, and P. F. Devaux. 2005. Reinvestigation by phosphorus NMR of lipid distribution in bicelles. *Biophys. J.* 88:1887–1901.
- Harroun, T. A., M. Koslowsky, M. P. Nieh, C. F. de Lannoy, V. A. Raghunathan, and J. Katsaras. 2005. Comprehensive examination of mesophases formed by DMPC and DHPC mixtures. *Langmuir*. 21:5356–5361.
- Van Dam, L., G. Karlsson, and K. Edwards. 2006. Morphology of magnetically aligning DMPC/DHPC aggregates—perforated sheets, not disks. *Langmuir*. 22:3280–3285.
- Tjandra, N., and A. Bax. 1997. Direct measurement of distances and angles in biomolecules by NMR in a dilute liquid crystalline medium. *Science*. 278:1111–1114.
- Ulmer, T. S., B. E. Ramirez, F. Delaglio, and A. Bax. 2003. Evaluation of backbone proton positions and dynamics in a small protein by liquid crystal NMR spectroscopy. *J. Am. Chem. Soc.* 125:9179–9191.
- Fleming, K., and S. Matthews. 2004. Media for studies of partially aligned states. *Methods Mol. Biol.* 278:79–88.
- Ketchem, R. R., W. Hu, and T. A. Cross. 1993. High-resolution conformation of gramicidin A in a lipid bilayer by solid-state NMR. *Science*. 261:1457–1460.
- Nevzorov, A. A., M. F. Mesleh, and S. J. Opella. 2004. Structure determination of aligned samples of membrane proteins by NMR spectroscopy. *Magn. Reson. Chem.* 42:162–171.
- Sanders 2nd, C. R., and G. C. Landis. 1995. Reconstitution of membrane proteins into lipid-rich bilayered mixed micelles for NMR studies. *Biochemistry*. 34:4030–4040.
- Czerski, L., and C. R. Sanders. 2000. Functionality of a membrane protein in bicelles. *Anal. Biochem.* 284:327–333.
- Fanucci, G. E., J. Y. Lee, and D. S. Cafiso. 2003. Membrane mimetic environments alter the conformation of the outer membrane protein BtuB. *J. Am. Chem. Soc.* 125:13932–13933.
- Howard, K. P., and S. J. Opella. 1996. High-resolution solid-state NMR spectra of integral membrane proteins reconstituted into magnetically oriented phospholipid bilayers. *J. Magn. Reson. B*. 112:91–94.
- Prosser, R. S., V. B. Volkov, and I. V. Shyanovskaya. 1998. Novel chelate-induced magnetic alignment of biological membranes. *Biophys. J.* 75:2163–2169.
- Glover, K. J., J. A. Whiles, M. J. Wood, G. Melacini, E. A. Komives, and R. R. Vold. 2001. Conformational dimorphism and transmembrane orientation of prion protein residues 110–136 in bicelles. *Biochemistry*. 40:13137–13142.
- De Angelis, A. A., A. A. Nevzorov, S. H. Park, S. C. Howell, A. A. Mrse, and S. J. Opella. 2004. High-resolution NMR spectroscopy of membrane proteins in aligned bicelles. *J. Am. Chem. Soc.* 126:15340–15341.
- Williamson, P. T., G. Zandomenighi, F. J. Barrantes, A. Watts, and B. H. Meier. 2005. Structural and dynamic studies of the gamma-M4 trans-membrane domain of the nicotinic acetylcholine receptor. *Mol. Membr. Biol.* 22:485–496.

33. Marcotte, I., and M. Auger. 2005. Bicelles as model membranes for solid and solution-state NMR studies of membrane peptides and proteins. *Concepts Magn. Reson.* 24A:17–37.
34. Marcotte, I., A. Belanger, and M. Auger. 2005. The orientation effect of gramicidin A on bicelles and Eu(3+)-doped bicelles as studied by solid-state NMR and FT-IR spectroscopy. *Chem. Phys. Lipids.* 139: 137–149.
35. Triba, M. N., M. Zoonens, J. L. Popot, P. F. Devaux, and D. E. Warschawski. 2006. Reconstitution and alignment by a magnetic field of a beta-barrel membrane protein in bicelles. *Eur. Biophys. J.* 35:268–275.
36. Ottiger, M., and A. Bax. 1999. Bicelle-based liquid crystals for NMR-measurement of dipolar couplings at acidic and basic pH values. *J. Biomol. NMR.* 13:187–191.
37. Cavagnero, S., H. J. Dyson, and P. E. Wright. 1999. Improved low pH bicelle system for orienting macromolecules over a wide temperature range. *J. Biomol. NMR.* 13:387–391.
38. Struppe, J., J. A. Whiles, and R. R. Vold. 2000. Acidic phospholipid bicelles: a versatile model membrane system. *Biophys. J.* 78:281–289.
39. Whiles, J. A., K. J. Glover, R. R. Vold, and E. A. Komives. 2002. Methods for studying transmembrane peptides in bicelles: consequences of hydrophobic mismatch and peptide sequence. *J. Magn. Reson.* 158:149–156.
40. Aussenac, F., B. Lavigne, and E. J. Dufourc. 2005. Toward bicelle stability with ether-linked phospholipids: temperature, composition, and hydration diagrams by ^2H and ^{31}P solid-state NMR. *Langmuir.* 21:7129–7135.
41. Lee, A. G. 1977. Lipid phase transitions and phase diagrams. II. Mixtures involving lipids. *Biochim. Biophys. Acta.* 472:285–344.
42. van Dijk, P. W., A. J. Kaper, H. A. Oonk, and J. de Gier. 1977. Miscibility properties of binary phosphatidylcholine mixtures. A calorimetric study. *Biochim. Biophys. Acta.* 470:58–69.
43. Feigenson, G. W., and J. T. Buboltz. 2001. Ternary phase diagram of dipalmitoyl-PC/dilauroyl-PC/cholesterol: nanoscopic domain formation driven by cholesterol. *Biophys. J.* 80:2775–2788.
44. Shimshick, E. J., and H. M. McConnell. 1973. Lateral phase separation in phospholipid membranes. *Biochemistry.* 12:2351–2360.
45. Mabrey, S., and J. M. Sturtevant. 1976. Investigation of phase transitions of lipids and lipid mixtures by sensitivity differential scanning calorimetry. *Proc. Natl. Acad. Sci. USA.* 73:3862–3866.
46. Dubois, M., L. Belloni, T. Zemb, B. Demé, and T. Gulik-Krzywicki. 2000. Formation of rigid nanodiscs: edge formation and molecular separation. *Prog. Colloid Polym. Sci.* 115:238–242.
47. Sternin, E., D. Nizza, and K. Gawrisch. 2001. Temperature dependence of DMPC/DHPC mixing in a bicellar solution and its structural implications. *Langmuir.* 17:2610–2616.
48. Hare, B. J., J. H. Prestegard, and D. M. Engelman. 1995. Small angle x-ray scattering studies of magnetically oriented lipid bilayers. *Biophys. J.* 69:1891–1896.
49. Seelig, J., and J. L. Browning. 1978. General features of phospholipid conformation in membranes. *FEBS Lett.* 92:41–44.
50. Israelachvili, J. 1985. Intermolecular and Surface Forces. Academic Press, London.
51. Lin, T.-L., S.-H. Chen, N. E. Gabriel, and M. F. Roberts. 1986. Use of small-angle neutron scattering to determine the structure and interaction of dihexanoylphosphatidylcholine micelles. *J. Am. Chem. Soc.* 108:3499–3507.
52. Minto, R. E., P. R. Adhikari, and G. A. Lorigan. 2004. A ^2H solid-state NMR spectroscopic investigation of biomimetic bicelles containing cholesterol and polyunsaturated phosphatidylcholine. *Chem. Phys. Lipids.* 132:55–64.
53. Curatolo, W., B. Sears, and L. J. Neuringer. 1985. A calorimetry and deuterium NMR study of mixed model membranes of 1-palmitoyl-2-oleylphosphatidylcholine and saturated phosphatidylcholines. *Biochim. Biophys. Acta.* 817:261–270.
54. Holmes, M. C., A. M. Smith, and M. S. Leaver. 1993. A small angle neutron scattering study of the lamellar phase of caesium pentadecafluorooctanoate (CsPFO)/1H–1H-perfluoroheptan-1-ol/ $^2\text{H}_2\text{O}$. *J. Phys. II.* 3:1357–1370.
55. Picard, F., M. J. Paquet, J. Levesque, A. Belanger, and M. Auger. 1999. ^{31}P NMR first spectral moment study of the partial magnetic orientation of phospholipid membranes. *Biophys. J.* 77:888–902.
56. Arnold, A., T. Labrot, R. Oda, and E. J. Dufourc. 2002. Cation modulation of bicelle size and magnetic alignment as revealed by solid-state NMR and electron microscopy. *Biophys. J.* 83:2667–2680.
57. Lindblom, G., K. Larsson, L. Johansson, K. Fontell, and S. Forsen. 1979. The cubic phase of monoglyceride-water systems. Arguments for a structure based upon lamellar bilayer units. *J. Am. Chem. Soc.* 101:5465–5470.
58. Holmes, M. C., P. Sotta, Y. Hendrikx, and B. Deloche. 1993. Water self diffusion in caesium pentadecafluorooctanoate (CsPFO)/ H_2O and CsPFO/CsCl/ H_2O and its relationship to structure. *J. Phys. II.* 3:1735–1746.
59. Soong, R., and P. M. Macdonald. 2005. Lateral diffusion of PEG-lipid in magnetically aligned bicelles measured using stimulated echo pulsed field gradient ^1H NMR. *Biophys. J.* 88:255–268.
60. Soong, R., and P. M. Macdonald. 2005. Influence of the long-chain/short-chain amphiphile ratio on lateral diffusion of PEG-lipid in magnetically aligned lipid bilayers as measured via pulsed-field-gradient NMR. *Biophys. J.* 89:1850–1860.
61. Rommel, E., F. Noack, P. Meier, and G. Kothe. 1988. Proton spin relaxation dispersion studies of phospholipid membranes. *J. Phys. Chem.* 92:2981–2987.
62. Triba, M. N. 2003. Etude physico-chimique des bicelles par RMN du phosphore-31. PhD thesis. Université Denis Diderot, Paris.
63. Bolze, J., T. Fujisawa, T. Nagao, K. Norisada, H. Saitô, and A. Naito. 2000. Small angle x-ray scattering and ^{31}P NMR studies on the phase behavior of phospholipid bilayered mixed micelles. *Chem. Phys. Lett.* 329:215–220.
64. Markvoort, A. J., K. Pieterse, M. N. Steijaert, P. Spijker, and P. A. J. Hilbers. 2005. The bilayer-vesicle transition is entropy driven. *J. Phys. Chem. B.* 109:22649–22654.
65. Small, D. M. 1986. The Physical Chemistry of Lipids: From Alkanes to Phospholipids. Plenum Press, New York. 489–500.

Supplementary material

Effects of lipid chain length and unsaturation on bicelles stability. A phosphorus NMR study

Mohamed N. Triba, Philippe F. Devaux, and Dror E. Warschawski*.

Unité Mixte de Recherche No. 7099, Centre National de la Recherche Scientifique, Institut de Biologie Physico-Chimique, Paris, France.

* to whom correspondence should be addressed : Dror E. Warschawski, Institut de Biologie Physico-Chimique, 13 rue Pierre et Marie Curie, 75005 Paris France
Telephone: 33 1 58 41 51 11. Fax: 33 1 58 41 50 24
E-mail: Dror.Warschawski@ibpc.fr

Lipid affinity for edges and bending energy involved in forming one edge.

When using a disk model or a perforated lamellae model, the bending energy per surface unity involved in forming one edge is estimated using the following expression (1):

$$E_b = \frac{k_c}{2A} \int_{x_{\min}}^{x_{\max}} [c_p(x) + c_m(x) - 2c_o]^2 dA$$

Where k_c and c_o are respectively the bending modulus and the spontaneous curvature (approximated as the average curvature at the hydrophilic/hydrophobic interface of a pure D6PC micelle, $c_o = 92 \times 10^{-3} \text{ \AA}^{-1}$) of the D6PC monolayer. $2A$ is the edge hydrophobic surface (approximated as the neutral surface) and $c_p(x)$ and $c_m(x)$ the principal curvatures for a surface element dA situated at a distance x from the symmetry axis (see Fig. S1). For a pore, x_{\min} and x_{\max} are respectively equal to $(R_p - e)$ and R_p while, for a disk edge, they are respectively equal to R_d and $(R_d + e)$, where R_p , R_d and e are respectively the pore radius, the disk radius and the edge thickness. $c_p(x)$, $c_m(x)$, dA and A are calculated using the following expressions (2).

$$c_p(x) = \frac{\sin\theta(x)}{x}; c_m(x) = \cos\theta(x) \frac{d\theta(x)}{dx}; dA = \frac{2\pi x}{\cos\theta(x)} dx \text{ and } A = \int_{x_{\min}}^{x_{\max}} dA.$$

While the angle $\theta(x)$ between the bilayer plane and the tangential plane at the hydrophilic/hydrophobic interface is given by :

$$\tan\theta(x) = \frac{a}{2e}(x - R) [e^2 - (x - R)^2]^{-\frac{1}{2}}$$

In this equation, a is the bilayer hydrophobic thickness, R corresponds to R_p for a pore and to R_d for a disk edge.

If the edge hydrophobic thickness e is taken as the fully extended hydrocarbon chains length of D6PC (7.8 \AA (3)), then the calculation indicates that for a given edge hydrophobic thickness e , E_b decreases as the bilayer hydrophobic thickness a decreases. Thus, by using D12PC instead of D14PC, D6PC affinity for edges should increase. On the contrary, this affinity should be reduced if D16PC is used instead of D14PC.

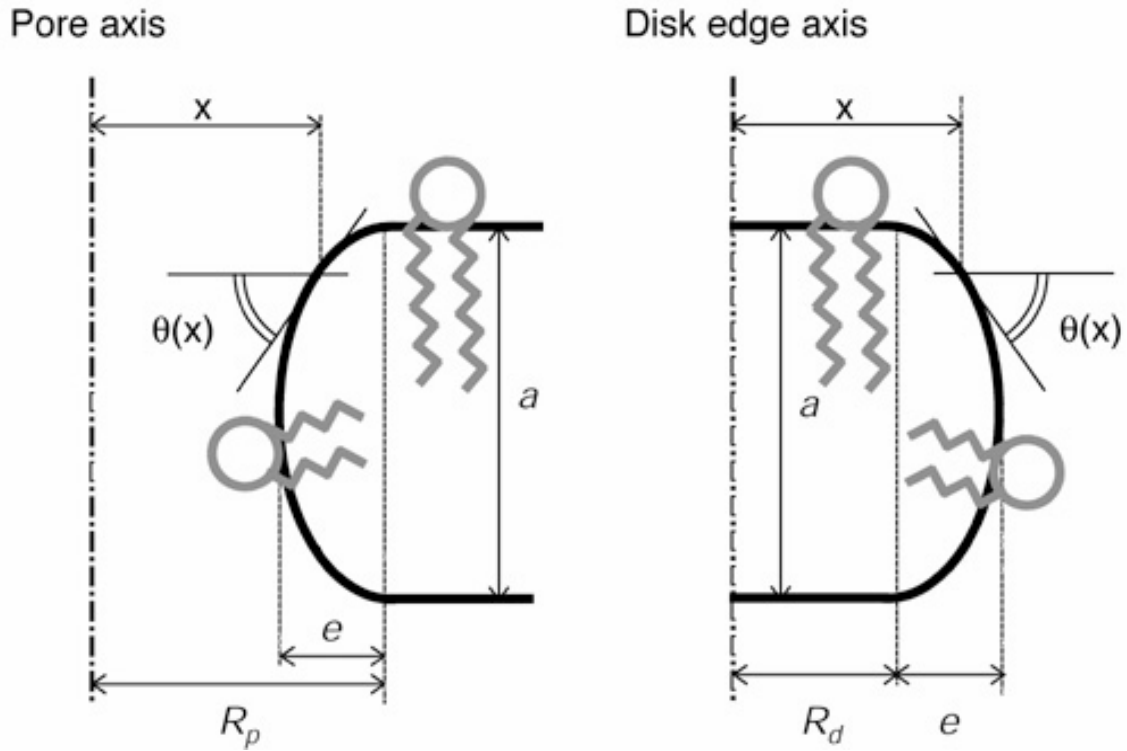


Figure S1. Schematic representation of the hydrophilic/hydrophobic interface in a pore and in a disk edge.

Pore radius.

The expressions presented here are based on two hypotheses assumed in different works in which perforated lamellae were proposed as the structural model for the temperature and composition domains where spontaneous alignment is observed. These hypotheses have also been assumed in the studies of other perforated bilayer structures (7). The first hypothesis is to consider a homogenous sample. Nieh *et al.* have shown that, in this case, the volume fraction of lipids in a perforated lamella is simply related to the repetitive distance $d_{//}$ between the lamellae (8,9). The second hypothesis consists in considering a uniform size of pores. Assuming this, Soong and Macdonald have shown that there is a simple relation between the pore radius R_p and the surface ratio between bilayers and edges (10). Assuming the same hypotheses, we have obtained an analytical expression of the pore radius R_p that can be used to discuss the validity of the perforated model. On Fig. 6, we define the bilayer thickness ($2r_{//}$), the edge thickness (r_{\perp}), the distance between pores (d_p) and the repetitive distance between the stacked bilayers ($d_{//}$). The volume fraction of lipids in the sample is ϕ .

If q_v is the ratio of the volume occupied by the bilayers in the sample, $V_{bilayer}$, divided by the volume occupied by the edges in the sample, V_{edge} , then:

$$q_v = \frac{V_{bilayer}}{V_{edge}} \quad (S1)$$

Let us call $S_{lamellae}$ the surface of all the perforated lamellae in the sample. We have:

$$S_{lamellae} = \frac{N_p}{\sigma_p} \quad (S2)$$

where σ_p is the surface density of pores and N_p is the number of pores in the sample. The volume occupied by the perforated lamellae $V_{lamellae}$ is given by:

$$V_{lamellae} = 2r_{||}S_{lamellae} \quad (S3)$$

We also define the volume fraction of lipids in the perforated lamellae f_l .

$$f_l = \frac{V_{bilayer} + V_{edge}}{V_{lamellae}} \quad (S4)$$

The volume occupied by the bilayer $V_{bilayer}$ is given by:

$$V_{bilayer} = 2r_{||}(S_{lamellae} - N_p\pi R_p^2) \quad (S5)$$

The volume occupied by the edges V_{edge} is given by :

$$V_{edge} = N_p V_{toroid} = N_p \pi r_{||} r_{\perp} \left(\pi R_p - \frac{4}{3} r_{\perp} \right) \quad (S6)$$

Where V_{toroid} is the volume of the inner toroidal annulus of a pore.

Introducing Eqs. S2, S5 and S6 into Eq. S1, we obtain a first relation between R_p and σ_p :

$$\frac{1}{\pi\sigma_p} = R_p^2 + \frac{\pi q_v r_{\perp}}{2} R_p - \frac{2q_v r_{\perp}^2}{3} \quad (S7)$$

Introducing Eqs. S2, S3, S5 and S6 into Eq. S4, we obtain a second relation between R_p and σ_p :

$$\frac{1}{\pi\sigma_p} = \frac{1}{(1-f_l)} \left(R_p^2 - \frac{\pi r_{\perp}}{2} R_p + \frac{2r_{\perp}^2}{3} \right) \quad (S8)$$

Equalizing expressions S7 and S8, we obtain a second order equation of R_p that can be easily resolved:

$$R_p = \frac{r_{\perp}}{4f_l} \left[1 + q_v(1-f_l) \right] \left(\pi + \sqrt{\pi^2 - \frac{32f_l}{3[1+q_v(1-f_l)]}} \right) \quad (S9)$$

Bolze and coworkers have experimentally determined $d_{||}$ by small angle X ray scattering for the D14PC/D6PC mixture at conditions for which alignment is observed ($q = 3$, $\phi_l \approx c_1 = 0.24$, and $T = 40^\circ\text{C}$) (11). The evolution of Bragg peaks obtained by these authors indicates that when alignable structures are formed, $d_{||}$ is almost temperature independent.

Nieh *et al.* have shown that in an homogeneous sample of perforated lamellae, f_l is given by (8):

$$f_l = \frac{d_{||}\phi_l}{2r_{||}} \quad (S10)$$

Where ϕ_l is the volume fraction of lipids in the sample and $d_{||}$ is the repetitive distance between the perforated lamellae.

R_p was calculated by using Eqs. S9 and S10. The various parameters have the following values: $d_{||} = 76 \text{ \AA}$ (11); $\varepsilon = 0.1$ (4); $2r_{||} = 44.2 \text{ \AA}$ (12); $\lambda = 0.61$ (13); $r_{\perp} = 16.8 \text{ \AA}$, by considering totally extended hydrophobic chains for D6PC (7.8 \AA , (3)) and an identical thickness of the hydrophilic domain for the edge and for the bilayer section (9 \AA , (12)). We find a pore radius R_p of 416 \AA .

Distance between pores.

We can estimate the average distance d_p between pores by considering that they are distributed in an hexagonal lattice. In this case the distance between the edges of two neighboring pores is:

$$d_p = \left(\sigma_p \sin \frac{\pi}{3} \right)^{\frac{1}{2}} - 2R_p \quad (\text{S11})$$

Using the same parameter values, we find a distance d_p between pores of 170 Å.

Disk radius.

In our previous work we have proposed a new method to estimate the bicelle radius based on the use of lipid volumes instead of lipid surface areas (4). This stems from the fact that lipid volumes are well known and do *not* depend on the aggregate curvature. In addition, to take into account the fact that the totally extended D6PC chains are 9 Å shorter than the totally extended D14PC chains, we also proposed an elliptical instead of a circular cross section for edges. Doing this, we clearly demonstrated that the bicelle radius strongly depends on the shape of its edge since this shape determines the available volume per bicelle for the short chain lipids.

Recently, a new formula has been proposed to estimate the disc radius (5). This new formula depends on the average surface s_s occupied by a short chain lipid at the hydrophobic interface between the edge domain and the bilayer domain, and it is supposed not to depend on edge shape. However, this parameter has not been determined experimentally for this lipidic system and the value used by Andersson and Måler is obtained essentially by simulation at the rigid hydrophobic interface of a protein. The extrapolation toward a lipid/lipid, hydrophobic, flexible interface can be questioned. Furthermore, assuming that lipid chains are incompressible (6), the model of Andersson and Måler imposes an edge that would imply the interfacial short chain lipids to be more extended than the long chain lipids. This result is unrealistic and it is probably a consequence of the large underestimation of s_s . The new formula proposed by Andersson and Måler introduces a new parameter, s_s , which is unmeasured experimentally, very difficult to estimate for the lipidic system studied here and, because of lipids incompressibility, also dependent on the edge shape.

Therefore, the disk radius R_d is given by :

$$R_d = \frac{1}{4} q_v r_{\perp} \left(\pi + \sqrt{\pi^2 + \frac{32}{3q_v}} \right) \quad (\text{S12})$$

Distance between disks.

Here again we suppose that the sample is composed of stacked lamellae. However each lamella consists of individual bicelles arranged onto a plane. By using a similar approach than previously, we can estimate the average distance between the edges of two neighboring disks.

Using expressions of the disk volume determined in our previous report (4), it is easy to show that the surface density of disk in each stacked plane is given by:

$$\sigma_d = \frac{2f_l}{\pi} \left[2R_d^2 + r_\perp \left(\pi R_d + \frac{4}{3} r_\perp \right) \right]^{-1} \quad (\text{S13})$$

where the volume fraction f_l of lipids in the plane and the disk radius R_d are given by Eqs. S10 and S12.

We can estimate the average distance d_d between disks by considering that they are distributed in a hexagonal lattice. In this case the distance between the edges of two neighboring disks is:

$$d_d = \left(\sigma_d \sin \frac{\pi}{3} \right)^{-\frac{1}{2}} - 2(R_d + r_\perp) \quad (\text{S14})$$

Using the same parameter values, we find a disk radius R_d of 260 Å and an average distance d_d of 256 Å between edges of two neighboring disks.

If one approximates the lateral diffusion of these bicelles by the lateral diffusion of a sphere of 260 Å radius, the time t needed for a bicelle to diffuse until it collides with the closest neighbour is given by $t = d_d^2 / (2D)$, where D is the diffusion coefficient, obtained using the Stokes-Einstein equation $D = k_B T / (6\pi\eta R_d)$, $k_B T = 4.3 \times 10^{-21}$ J is the thermal energy and $\eta = 10^{-3}$ kg m⁻¹ s⁻¹ is the viscosity of water. We find that $t \approx 0.04$ ms.

Bicelles for biological applications.

Soluble proteins.

Today, bicelles are essentially used for the study of *soluble* proteins. The alignment quality of standard bicelles is sufficient, although it is convenient to be able to perform the NMR experiments under several orientation qualities with the same sample (14,15). In addition, working with standard D14PC/D6PC bicelles requires a temperature of 40°C which is very high for protein stability. Experiments could be performed between 10 and 50°C if using binary mixtures made of D12PC/D6PC:3/1 rather than the usual D14PC/D6PC:3/1 mixture. In addition, since the quality of alignment improves when raising the temperature, performing the NMR experiments on the same sample, at several different temperatures in this range would provide more information to resolve structural ambiguities.

Membrane proteins.

For *membrane* proteins, the bilayer composition should be similar to the lipidic composition of biological membranes. For this purpose, we have shown that the nature of the long chain lipids could be varied, keeping in mind that miscibility between lipids is the important parameter to follow. We have shown for example that an alignable sample can be obtained with up to 50% POPC in the bilayer (Fig. 3b). The presence of detergents in the bilayer can affect a membrane protein reconstituted in bicelles. A way to reduce this effect is to reduce the miscibility between the long and the short chain lipids. For example, for a

bicelle that contains D14PC as long chain lipid, the use of D5PC instead of D6PC or D7PC will reduce the interactions between detergents and the membrane protein.

To obtain a good spectral resolution, a high level of alignment has to be reached and we believe that bicellar system may have suffered from a slightly insufficient alignment quality so far (compared to glass plates). In order to improve the bicelle alignment, ^{31}P NMR indicates that one should increase either the proportion q of long chain lipids in the sample (Fig. 1a vs. Fig. 1b) or the chain length of the short chain lipids (Fig. 1a vs. Fig. 1c). The best possible alignment for a given lipidic composition occurs at a sample temperature just below T_v , the temperature where perforated vesicles appears. To avoid protein unfolding, alignment should take place at reasonable temperatures and T_v can be reduced by replacing a fraction of the long chain lipids by unsaturated lipids such as POPC.

For membrane protein studies, it is preferable to have the bicelle normal *parallel* to the magnetic field. This alignment is reached by addition of lanthanide ions. Lanthanide ions bind to phospholipids and, at high concentration, they can induce a structural change of the bicellar aggregate. However, in presence of only 1% lanthanide chelates in the bilayer, the value of the lanthanide/lipid molar ratio is highly reduced (< 0.01). In these conditions, lanthanides are largely sequestered by the chelates molecules and no change is observed in the order parameter profile of the long chain lipids. Furthermore, with low lanthanide concentration, the quadrupolar splitting simply increases by a factor 2, suggesting that the lipidic aggregates are only flipped by 90° and that no changes occur in lipidic structures and in their interactions (16-18). Consequently, it is very likely that most of the experimental results we present in this report should also be true in presence of the small amount of lanthanides necessary for the study of membrane proteins.

Finally, the protein itself can affect the properties of the bicelle it is reconstituted into. While little data on this subject is available, we have discussed the effect of α -helical vs. β -barrel proteins on bicelles alignment properties in a previous article (19). These effects are hardly predictable but recent results show that proteins are aligned in presence of lipid mixtures and lanthanides, in a temperature range where the same lipidic mixture would align without the protein (see (19) and references therein).

In conclusion, for membrane protein studies, the bicelle lipidic system can be tailored to reach various purposes: D14PC/D7PC:5/1 mixtures at 29°C provide the best alignment possible at a reasonable working temperature but D14PC/D5PC:5/1 mixtures at 37°C are preferred if one wants to reduce the amount of detergent-like molecules in the bilayer domains.

Drug encapsulation and delivery.

It has been suggested that bicellar systems could also be used for drug encapsulation and delivery (20). In the classical mixture, a transition from perforated to closed vesicles occurs at body temperature for D14PC/D6PC:10/1(4). The same transition could also be obtained with a lower q ratio if changing the short-chain lipid. For example, this transition is observed in D14PC/D7PC:6/1, as seen on Fig. 1d.

SUPPLEMENTARY MATERIAL REFERENCES

1. Dubois, M., V. Lizunov, A. Meister, T. Gulik-Krzywicki, V. J. Marc, E. Perez, J. Zimmerberg, and T. Zemb. 2004. Shape control through molecular segregation in giant surfactant aggregates. *Proc. Natl. Acad. Sci. U. S. A.* 101:15082-15087.
2. Markin, V. S. and J. P. Albanesi. 2002. Membrane fusion: stalk model revisited. *Biophys. J.* 82:693-712.
3. Tanford, C. 1991. *The hydrophobic effect: formation of micelles and biological membranes.* New York, NY.: John Wiley and Sons.
4. Triba, M. N., D. E. Warschawski, and P. F. Devaux. 2005. Reinvestigation by phosphorus NMR of lipid distribution in bicelles. *Biophys. J.* 88:1887-1901.
5. Andersson, A. and L. Maler. 2005. Magnetic resonance investigations of lipid motion in isotropic bicelles. *Langmuir* 21:7702-7709.
6. Israelachvili, J. 1985. *Intermolecular & Surface Forces.* A. Press, editor. London: Academic Press.
7. Holmes, M. C., A. M. Smith, and M. S. Leaver. 1993. A small angle neutron scattering study of the lamellar phase of caesium pentadecafluorooctanoate (CsPFO)/1H-1H-perfluoroheptan-1-ol/²H₂O. *J. Phys. II* 3:1357-1370.
8. Nieh, M. P., C. J. Glinka, S. Krueger, R. S. Prosser, and J. Katsaras. 2001. SANS study on the structural phases of magnetically alignable lanthanide-doped phospholipid mixtures. *Langmuir* 17:2629-2638.
9. Nieh, M. P., C. J. Glinka, S. Krueger, R. S. Prosser, and J. Katsaras. 2002. SANS study on the effect of lanthanide ions and charged lipids on the morphology of phospholipid mixtures. *Biophys. J.* 82:2487-2498.
10. Soong, R. and P. M. Macdonald. 2005. Influence of the long-chain/short-chain amphiphile ratio on lateral diffusion of PEG-lipid in magnetically aligned lipid bilayers as measured via pulsed-field-gradient NMR. *Biophys. J.* 89:1850-1860.
11. Bolze, J., T. Fujisawa, T. Nagao, K. Norisada, H. Saitô, and A. Naito. 2000. Small angle X-ray scattering and ³¹P NMR studies on the phase behavior of phospholipid bilayered mixed micelles. *Chem. Phys. Lett.* 329:215-220.
12. Nagle, J. F. and S. Tristram-Nagle. 2000. Structure of lipid bilayers. *Biochim. Biophys. Acta* 1469:159-195.
13. Small, D. M. 1986. *The physical chemistry of lipids: from alkanes to phospholipids.* D. M. Small, editor. New York: Plenum Press. 489-500 p.
14. Lancelot, N., K. Elbayed, and M. Piotto. 2005. Applications of variable-angle sample spinning experiments to the measurement of scaled residual dipolar couplings and ¹⁵N CSA in soluble proteins. *J. Biomol. NMR* 33:153 - 161.
15. Lakomek, N. A., T. Carlomagno, S. Becker, C. Griesinger, and J. Meiler. 2006. A thorough dynamic interpretation of residual dipolar couplings in ubiquitin. *J. Biomol. NMR* 34:101-115.
16. Prosser, R. S., J. S. Hwang, and R. R. Vold. 1998. Magnetically aligned phospholipid bilayers with positive ordering: a new model membrane system. *Biophys. J.* 74:2405-2418.
17. Prosser, R. S., V. B. Volkov, and I. V. Shiyankovskaya. 1998. Novel chelate-induced magnetic alignment of biological membranes. *Biophys. J.* 75:2163-2169.
18. Tiburu, E. K., P. C. Dave, and G. A. Lorigan. 2004. Solid-state ²H NMR studies of the effects of cholesterol on the acyl chain dynamics of magnetically aligned phospholipid bilayers. *Magn. Reson. Chem.* 42:132-138.

19. Triba, M. N., M. Zoonens, J. L. Popot, P. F. Devaux, and D. E. Warschawski. 2006. Reconstitution and alignment by a magnetic field of a beta-barrel membrane protein in bicelles. *Eur. Biophys. J.* 35:268-275.
20. Yue, B., C.-Y. Huang, M.-P. Nieh, C. J. Glinka, and J. Katsaras. 2005. Highly Stable Phospholipid Unilamellar Vesicles from Spontaneous Vesiculation: A DLS and SANS Study. *J. Phys. Chem. B* 109:609-616.